SEARCHING FOR NEW DUAL INHIBITORS OF CYCLOOXYGENASE 2 AND 5-LIPOXYGENASE – AN *IN SILICO* APPROACH

Divya. V[1*], Aswathy. S. Nair[2], Achutha A. S[3], V. L Pushpa[4], S. V Manoj[5]

Submitted: 10 May 2023 **Revised and Accepted : 12 June 2023** **Published Date : 20 July 2023**

Abstract

A novel method for producing NSAIDs is the use of COX-2/5-LOX dual inhibitors, which efficiently block inflammatory mediators from the cyclooxygenase and lipoxygenase pathways with fewer side effects. In the current work, 63 molecules with experimentally determined IC50 values for COX-2/5-LOX inhibition were collected and developed QSAR models. During the 2D QSAR study, one statistical model each were chosen for COX-2 inhibition ($R^2 = 0.9308$ and $Q^2 = 0.8936$) and for 5-LOX inhibition $R^2 = 0.9209$ and $Q^2 = 0.8879$). These models were used for virtual screening for finding out new COX-2/5-LOX new inhibitor leads. In addition, docking studies were performed to quantify the binding affinity of eligible query compounds towards COX-2 and 5-LOX proteins and to uncover the specific interactions that take place between ligands and the proteins. The pharmacodynamic and pharmacokinetic features revealed that molecules VS864, VS865, VS882, VS888, VS895, VS896, VS897, and VS898 said to be taken as best molecules without any hazardous impact, according to all current drug-likeness criteria. To ascertain the binding stabilities, molecular dynamic simulations of the hits were studied. As a result, these compounds can be evaluated as possible COX-2/5-LOX dual inhibitor candidates.

Keywords: COX-2/5-LOX dual inhibitors, QSAR, virtual screening, molecular docking, pharmacokinetic analysis, Molecular Dynamic simulations

[1, *2,]Department of Chemistry, Milad-E-Sherief Memorial College, Kayamkulam, University of Kerala, Kerala, PIN 690502, INDIA
[3,4,5]Sree Narayana College, Kollam, University of Kerala, Kerala, Kerala, PIN: 691001, INDIA

***Corresponding Author:** Divya. V
*Department of Chemistry, Milad-E-Sherief Memorial College, Kayamkulam, University of Kerala, Kerala, PIN 690502, INDIA

DOI: 10.53555/ecb/2023.12.7.372

Introduction

Traditional non-steroidal anti-inflammatory medicines, also known as NSAIDs, are one of the most widely used classes of medication in the world. These medications exert their analgesic and anti-inflammatory effects by blocking the manufacture of COX enzyme-associated inflammatory cytokines[1]. In the process that leads to the production of arachidonic acid (AA), COX is an essential enzyme. It contains two isoenzymes known as COX-1 and COX-2, both of which act as mediators in the process of converting arachidonic acid into prostaglandins[2]. Even though nonsteroidal anti-inflammatory drugs (NSAIDs) have been confirmed to be on the WHO Model List of Essential Medicines, they are associated with a number of potentially harmful side effects, including gastrointestinal toxicities, hepatotoxicity, cardiovascular risks, renal injuries, and stroke[3]. The pharmaceutical sector faces a problem when it comes to the development of nonsteroidal anti-inflammatory drugs (NSAIDs) that have an improved safety profile.

The binding site of COX-2 enzyme has a secondary pocket in addition to the primary pocket, which is not present in the COX-1 enzyme's binding site. This secondary pocket was created because of the substitution of the bulkier amino acid ILE523 in COX-1 with the more compact VAL523 in COX-2. Because of this, selective COX-2 inhibitors typically consist of bulky stiff groups that make it possible for additional binding interactions to take place inside COX-2 secondary pockets but prohibit the compound from fitting inside the smaller COX-1 channel. Blocking only COX-2 will shift the inflammatory pathway toward the LOX pathway, which will cause a greater number of side effects due to the increased generation of leukotrienes, which are involved in the inflammatory process[4].

5-lipoxygenase (5-LOX) is one of the three principal iso enzymes of liquid oxygen, and it plays a role in the metabolic process of AA.
Additionally, there is a compensating mechanism with COX[5]. Important mediators of inflammatory and allergy illnesses are leukotrienes (LTs), which are produced by the LOX pathway[6].

Compounds that inhibit both COX-2 and 5-LOX provide several benefits on their users. This is because they operate on both primary arachidonic acid metabolic pathways and exhibit a diverse array of anti-inflammatory properties. Dual inhibition of the COX-2/5-LOX enzyme creates a reasonable technique for the creation of novel anti-inflammatory drugs that have an excellent safety profile[789]. The development and investigation of a dual inhibitor is still desperately required in the market at this moment beginning[10]. Common drugs for inflammation are Celecoxib, Naproxen, Diclofenac, Indomethacin etc. are represented in Figure 1.
We must synthes
ize and screen several compounds to build a better analogue with the desired profile. Because the mechanism of action and the precise target with which these analogues interact are unclear, using computer assisted drug design (CADD) with the available data is a good technique for lead optimization[11]. As a result, in this study, a ligand-based drug design technique known as QSAR was used to identify structural properties that have a strong relationship with biological activity. In recent decades, CADD has emerged as a viable alternative to the traditional 'trial and error' drug design process for unravelling the secrets of structural patterns that regulate a drug candidate's activity, pharmacokinetics, and toxicity profiles[11–14]

.

a)

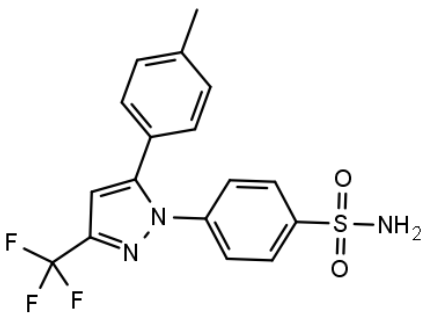

b)

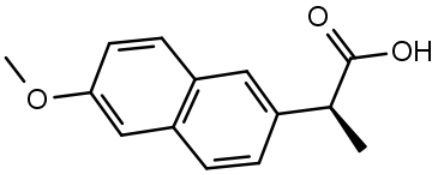

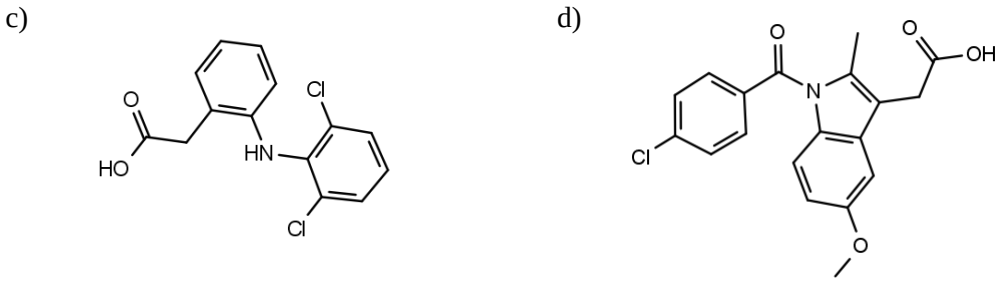

Figure 1: Structures of a) Celecoxib, b) Naproxen c) Diclofenac and d) Indomethacin

The main objective of the present work is the identification of novel COX-2/ 5-LOX dual inhibitor leads by the systematic utilization of QSAR models for virtual screening followed by pharmacodynamic and pharmacokinetic feature selections. For that we initially develop statistically robust and easily interpretable QSAR models. Using these models, virtually test a series of novel compounds whose activities against inflammation have not yet been identified. Following the completion of the virtual screening[15–18], the chosen compounds were sent to molecular docking with the COX-2 and 5-LOX proteins, which was then followed by a prediction of their pharmacokinetic properties.

Materials and methods

QSAR Model generation

In the current investigation, a dataset consisting of 63 molecules that possessed inhibitory activity toward COX-2 and 5-LOX was initially drawn on 2D sketcher before being converted into 3D structures with the help of the MMFF94 force field[19–23]. Their inhibitory activities were calculated using the pIC50 formula (pIC50=-logIC50) (IC50= Half-maximal inhibitory concentration). Because these molecules exhibit such a broad spectrum of activities (pIC50 values range from 7.678 to 3.945 for COX-2 and 6.6383 to 3.8844 for 5-LOX), the selection of these molecules for inclusion in the dataset is entirely warranted. The structures of all the molecules and their reported activity values IC50 and pIC50 are present in the supplementary materials (Appendix 1). PaDEL-Descriptor 2.18[24] produced 1D, 2D, and 3D molecular descriptors and fingerprints. More than 15000 molecular descriptors describe every molecule. To avoid the inclusion of redundant and collinear molecular descriptors in the development of a robust QSAR model, QSARINS-2.2.4 was used to remove constant, nearly constant and highly correlated (correlation greater than 0.90) molecular descriptors. This reduced molecular descriptors to 69. QSARINS-2.2.4[25,26] (http://www.qsar.it) was used to forecast models with improved predictive abilities and a defined application domain. 40 compounds were used for model creation and 12 for model validation. QSARINS-2.2.4 used GA-MLR (Genetic Algorithm-Multilinear Regression) to generate optimum models. Q^2_{LOO} was used as a fitness function to avoid overfitting and simplify the model. 10000 generations were set. According to OECD guidelines, the created models underwent internal and external statistical validation. Models with a high degree of predictability are discussed in detail.

Virtual Screening Based on QSAR model.

Using Schrodinger Software(2021-1)[27], Figure 2 structural template was used to produce 1022 variations for QSAR-based virtual screening. These molecules were used for QSAR based virtual screening. The three-dimensional structures of molecules were constructed in the same way as modelling sets before the molecular descriptor calculations were performed. Then, a proven QSAR model were utilised to predict new drugs' biological properties.

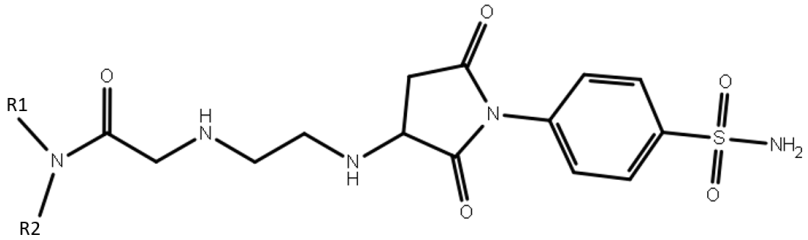

Figure 2: Template for enumerations.

Molecular Docking Analysis

The pdb file for cyclooxygenase- 2 receptor (PDB ID: 5KIR, resolution 2.70Å) was fetched from RCSB-PDB (https://www.rcsb.org/). Crystal structure of 5-LOX (PDB ID: 3O8Y, resolution 2.389Å) was retrieved from RCSB-PDB. The Ramachandran plot was utilised to evaluate the protein's quality (Figure 3). The presence of most residues in the preferred zone (shown by the red- and yellow-coloured regions) and only a few residues in the unfavourable region (represented by the white coloured region) validates the protein's suitability for docking investigations.

The simulations of molecular docking were carried out with the help of AutoDock-4.2.6, which was embedded into AutoDock Tools-1.5.6[28,29]. AutoDock tools were used to provide polar hydrogens and partial charges to the protein and ligand before the compounds were docked into the predetermined active site. Through docking of the reported drug molecules in the target protein, the location and size of the active region of the target protein, which is where substantial ligand-receptor interactions occur, were determined. A grid box of 60Å in size was constructed around the residues HIS90 and ARG513 (in the case of COX-2)[30] and around ILE406, TYR181, HIS600 and LEU420 (in the case of 5-LOX)[31]. The autodock software employs a grid-based algorithm that conducts an exhaustive search inside the binding site's dimensions. The autodock software employs a grid-based algorithm that conducts an exhaustive search inside the binding site's dimensions. The Lamarckian Genetic Algorithm (GA) was used to do research on the conformation of the ligand. The population size of the Genetic Algorithm was set to be 150, the number of GA evaluations was set to be 2500000, and the number of GA docking runs was set to 100. Each ligand was docked independently with enzymes to optimise binding. After docking, ligand binding energies at enzyme active sites were studied. By measuring the binding energies, H-bonding interactions, hydrophobic interactions, and van der Waal's interactions were examined.

a) b)

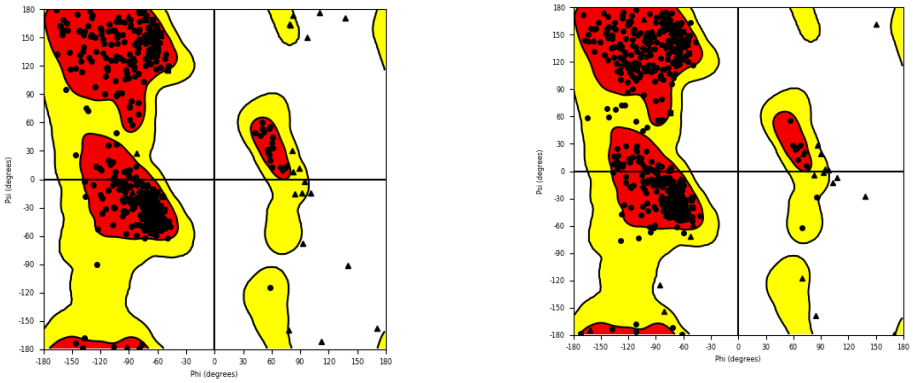

Figure 3: Ramachandran plot for a) cyclooxygenase- 2 receptor (PDB ID: 5KIR) and b) 5-lipoxygenese (PDB ID: 3O8Y)

Pharmacokinetic property study

Pharmacokinetic characteristics (ADMET)of all 18 virtually screened compounds were evaluated using ADMETLab 2.0[32], which has a stronger capacity to aid medicinal chemists in quickening the drug research and development process. For the pharmacokinetic property prediction, SMILES notations of each compound was employed.

Molecular Dynamic Simulations

All the MD simulations were done using the NAMD package (Version 2.14) developed by the Theoretical and Computational Biophysics Group in the Beckman Institute for Advanced Science and Technology at the University of Illinois at Urbana−Champaign with the CHARMM 36 force field[33]. The dynamic simulations were done using TIP3P water box with a padding of 5Å keeping temperature and pressure constant at 310 K and 1 atm respectively for 20ns. The preparation and analysis were carried out using VMD package 1.9.3 (available at http://www.ks.uiuc.edu/Research/vmd/)[34].

Result and Discussions

QSAR model generation and its validation

The Quantitative Structure-Activity Relationship (QSAR) has emerged as an intriguing approach for identifying the most important structural features

and predicting desired activity using a series of molecules. QSAR models were created by correlating easily interpretable chemical descriptors with structural characteristics. A good QSAR model quality is determined by its goodness of fit, robustness, and predictability. Following OECD criteria results in a reliable and reproducible QSAR. For QSAR model creation, 63 compounds with specified COX-2 and 5-LOX inhibition generated using the same bioassay approach were evaluated. These compounds are structurally similar and function in the same way.

QSARINS was used to run a multiple linear regression (MLR) analysis on the identified compounds. When the number of descriptors for running the genetic algorithm (GA) was set to 5, statistically meaningful MLR models were created. The following are the best GA-MLR models for COX-2 and 5-LOX:

GA-MLR QSAR Model for COX2 inhibitors

$$pIC50 = 1.0702(\pm 0.7660) + 0.2941(\pm 0.2678) * C1SP2 - 7.0059(\pm 2.5870) * MDEN12 + 0.6293(\pm 0.4786) * MLFER_A + 0.6567(\pm 0.1459) * nTRing + 0.3248(\pm 0.08) * nRotB$$

GA-MLR QSAR Model for 5-LOX inhibitors

$$pIC50 = 2.7443(\pm 0.3839) + 0.2358(\pm 0.0438) * nBondsD + 0.2572(\pm 0.1439) * C3SP2 + 0.7215(\pm 0.1153) * n6HeteroRing - 0.5564(\pm 0.3232) * PubchemFP192 + 0.3419(\pm 0.1945) * PubchemFP300$$

The performance of 2D QSAR model developed for COX-2 and 5-LOX were presented in table 1.

Table 1: Performance of 2D QSAR model developed by QSARINS for COX-2 and 5-LOX inhibitors.

Validation parameters	COX-2	5-LOX	Validation parameters	COX-2	5-LOX
R2	0.9308	0.9209	**CCC cv**	0.9452	0.9418
R2adj	0.9206	0.9068	**Q2 LMO**	0.8772	0.8791
LOF	0.13	0.1034	**R2 Yscr**	0.1255	0.1544
RMSE tr	0.2705	0.227	**Q2 Yscr**	-0.2462	-0.2564
MAE tr	0.2076	0.1816	**RMSE ext**	0.4648	0.2946
CCC tr	0.9641	0.9588	**MAE ext**	0.3066	0.181
s	0.2933	0.2502	**R2ext**	0.779	0.8575
F	91.4116	65.214	**Q2-F1**	0.7722	0.8492
Q2loo	0.8936	0.8879	**Q2-F2**	0.7326	0.8461
RMSE cv	0.3352	0.2703	**Q2-F3**	0.7955	0.8668
MAE cv	0.2537	0.2187	**CCC ext**	0.8781	0.9254

Figure 4 show the experimental versus projected pIC50 values for the COX-2 GA-MLR model as well as Williams plot to examine the application domain of the model and figure 5 shows the 5-LOX GA-MLR model as well as Williams the two models to examine the application domain of the model. Numerous developed QSAR models meet the specified threshold values for statistical parameters. The fact that the values for the, R^2 (coefficient of determination), R^2_{adj} (adjusted coefficient of determination), LOF (lack of fit), and R^2_{cv} (Q^2loo) (cross-validated coefficient of determination for leave-one out) are so close together demonstrates that the model contains the ideal number of variables and does not suffer from over-fitting. The high value of Q^2_{LMO} (Cross-validated coefficient of determination for leave-many-out) indicates that a model's internal validation is satisfactory. The low values of R^2_{Yscr} and Q^2_{Yscr} (Y scrambling related parameters) indicate that the constructed model is clear of random correlations. The high values of R^2_{ex} (external coefficient of determination), $Q^2 - F^n$ and CCC_{ex} (concordance correlation coefficient) show that the external predictive capacity is adequate. The F (Fischer F-ratio) value indicates how statistically significant the models are.

C1SP2 (Doubly bound carbon bound to one other carbon), *MDEN-12* (Molecular distance edge between all primary and secondary nitrogens), *MLFER_A* (Overall or summation solute hydrogen bond acidity), *nTRing* (Number of rings (includes counts from fused rings)) and *nRotB* (Number of rotatable bonds, excluding terminal bonds) were identified as the independent variables that influence COX-2 inhibitory activity. Positive coefficients imply an increase in projected activity, whereas negative coefficients suggest a decline.

5-LOX inhibitory activity was shown to be dependent on *nBondsD* (Number of double bonds), *C3SP2* (Doubly bound carbon bound to three other carbons), *n6HeteroRing* (Number of 6-membered rings containing heteroatoms (N, O, P, S, or halogens)), *PubchemFP192* (Any ring size 6 which does not share three consecutive atoms with any other ring in the chemical structure), and *PubchemFP300* (simple N-N atom pairs. These bits test for the presence of patterns of bonded atom pairs regardless of bond order or count).

Virtual Screening Based on QSAR model

Supplementary materials (Appendix 2) include the structures and estimated values of pIC50 for top 50 molecules (They are having predicted pIC50 value for COX-2 inhibition greater than 7.00**)** utilised for virtual screening. Molecules having an anticipated COX-2 inhibitory activity that was larger than 7.50 were chosen for the prediction of their 5-LOX inhibitory activity, docking analysis, and pharmacokinetic property investigations. This resulted in the selection of 18 different molecules. The 18 most active compounds, as predicted by the generated QSAR models (COX-2 and 5-LOX), are shown in the figure 6. According to the model, increasing the independent variables (except *MDEN-12* for which a decrease in the value will result in increased pIC50 value) proposed by the QSAR model equation for COX-2 inhibition could result in a higher pIC50 value for a molecule.

a)

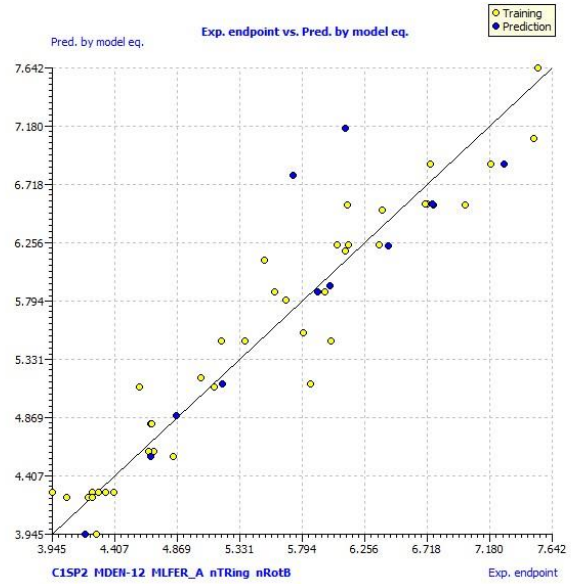

b)

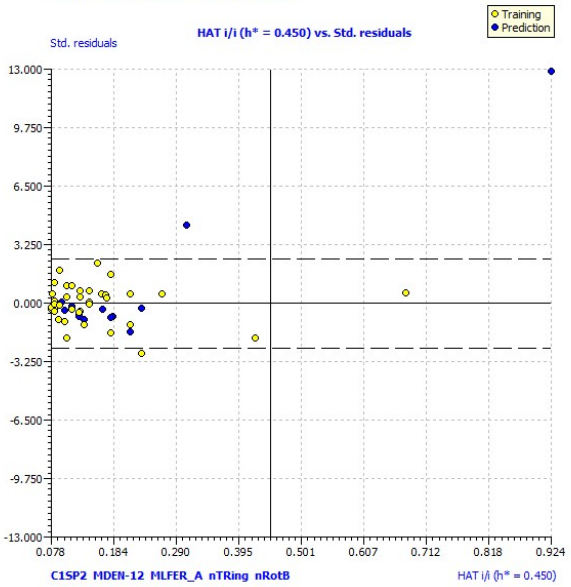

Figures 4: a) The experimental versus projected pIC50 values for the COX-2 GA-MLR model and b) Williams plot to examine the application domain of the model

a)

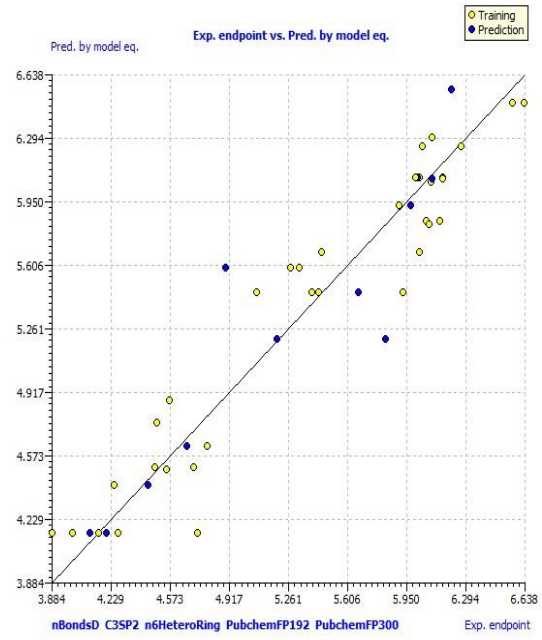

b)

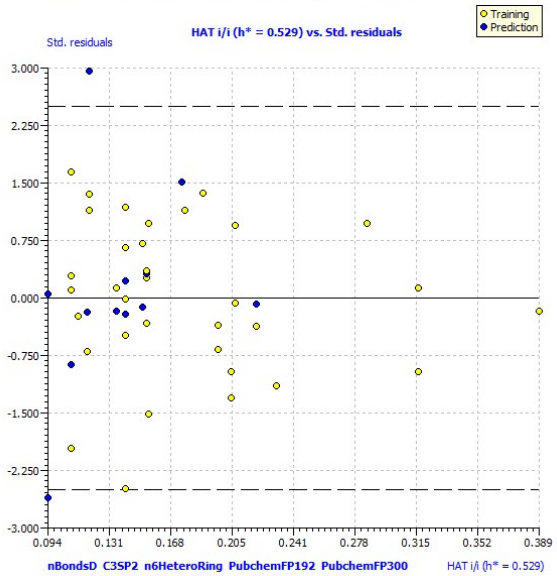

Figure 5: a) The experimental versus projected pIC50 values for 5-LOX GA-MLR model and b) Williams the two models to examine the application domain of the model.

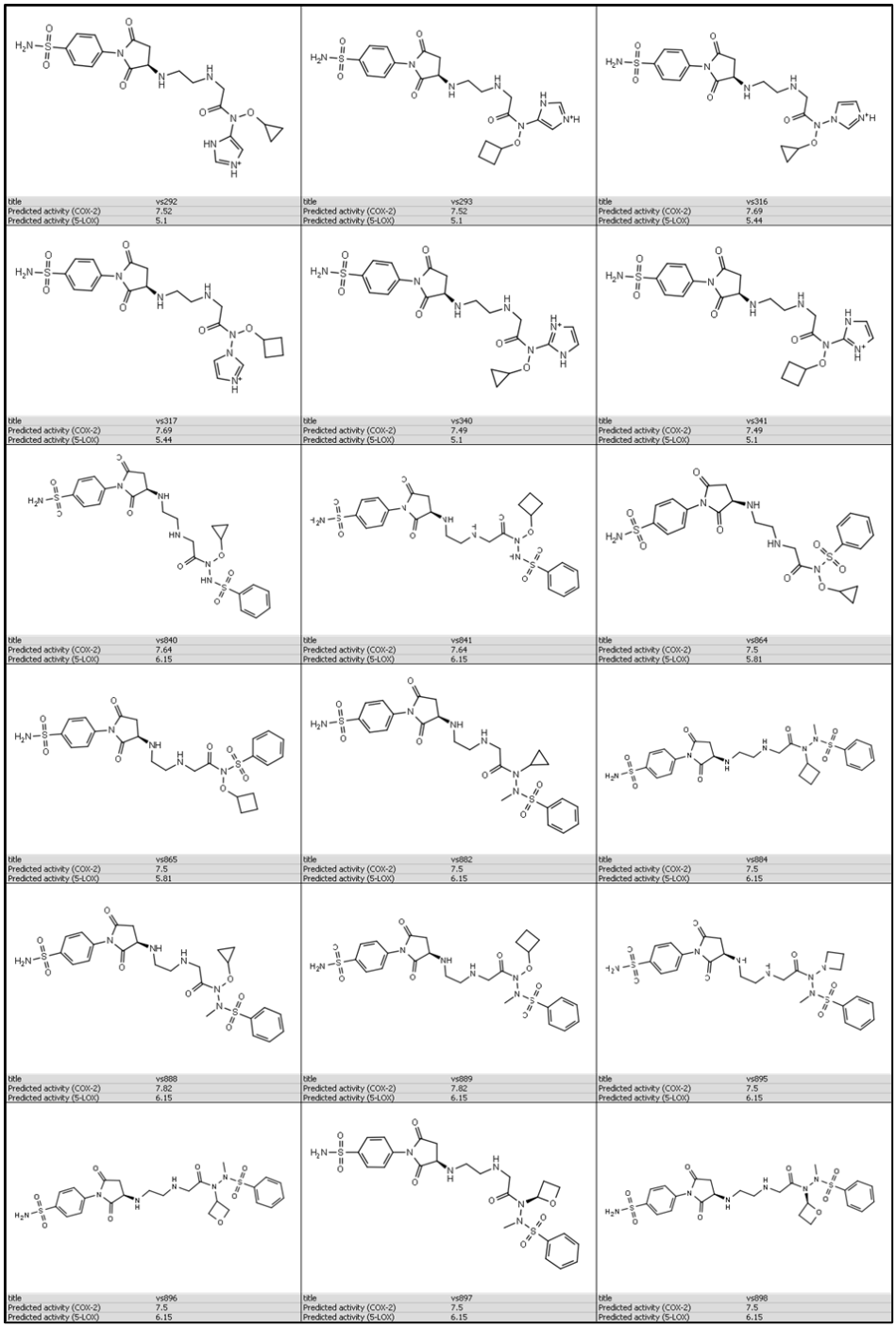

Figure 6: Structures and predicted pIC50 values (COX-2 and 5-LOX) of 18 virtually screened molecules

Molecular Docking Analysis

Molecular docking is a widely adopted structure-based drug development technique in CADD and is currently used as a powerful tool for predicting the bioactive conformation of molecules by specifying the key interacting residues, binding interactions, and scoring functions. Bioactive conformations of a molecule are stable conformations characterised by extremely negative binding energy. Docking a reference drug molecule, celecoxib (pIC50 =7.30) an approved COX-2 inhibitor, was used to identify the essential properties for an efficient COX-2 inhibition. 2D and 3D ligand interaction diagrams were presented in figure 7. After that, all the 18 molecules having pIC50 value greater than 7.50 obtained after virtual screening using the QSAR model for COX-2 were chosen for molecular docking by specifying the grid obtained after docking of reference molecule. The docking score and the interacting residues of celecoxib and 18 molecules were presented in table 2. We give the docking postures of VS865 and VS896 as illustrative instances. Their docking scores are respectively -9.76 kcal/mol and -9.66 kcal/mol (Figure 8).

Celecoxib produces hydrogen bonding contacts with SER353, ILE517, HIS90, GLN192, PHE518 and LEU352, amide-pi stacking hydrophobic interactions with LEU352, and alkyl or pi-alkyl hydrophobic interactions with LEU359, MET522, ALA527, TRP387, VAL523, VAL349, and PHE518. Because of these interactions, the celecoxib molecule's binding to the active site of COX-2 is made more stable, which results in a lower free energy of binding energy (-10.78 kcal/mol). While docking 18 virtually screened molecule, it was observed that except VS316 and VS340, the $-S = O$ oxygen of all other compounds form hydrogen bonding interactions with PHE518. The residues SER353, ILE517, GLN192, and LEU352 are also important contributors to the formation of hydrogen bonding connections with $-SO_2 - NH_2$ group of ligand molecules. Except VS292, VS293, VS316, VS340, VS884 and VS895, other 12 molecules form hydrogen bonding interactions with ARG120. All of the compounds demonstrated alkyl/pi-alkyl hydrophobic interactions with the protein, and the three residues VAL523, LEU93, and VAL89 were found to be the most important residues in these interactions. In addition to interactions involving hydrogen bonding and hydrophobic contacts involving alkyl/pi-alkyl, VS316 and VS340 have demonstrated the presence of pi-sulphur interactions with TRP387. Pi-cation interactions TYR181, TRP599, PHE421, ILE415, and HIS367. Figure 9 depicts 2D interaction graphs of Zileuton and VS865 with 5-LOX protein.

a)

b)

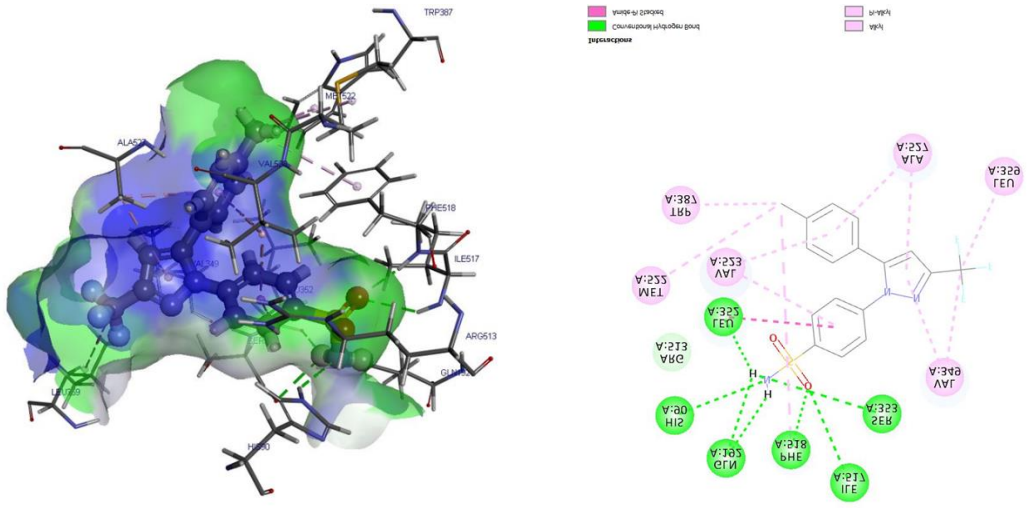

Figure 7: a)3D and b) 2D ligand interaction diagrams of Celecoxib with COX-2

Pharmacokinetic property predictions

The 18 compounds were then submitted to ADMETLab 2.0 for pharmacokinetic property prediction. Table 4 displays the results of the physiochemical qualities and medicinal properties have been seen between ARG120 and the pi-electron cloud of the phenyl ring in VS840, VS896 and VS889, which have estimated free binding energies of -9.13 and -9.76 kcal/mol, respectively. In the case of VS864 and VS896, the pi-electron cloud of the amide linkage that is present in LEU352 creates a hydrophobic connection with the pi-electron cloud of the benzene ring that is present in the ligand molecules. LEU352 and SER353 are the sites of the pi-sigma hydrophobic interactions formed by VS864 and VS889, respectively.

Molecular docking of these compounds was performed with 5-LOX protein in a manner analogous to that described above. The residues ILE406, PHE177, TYR181, THR364, ASN407, LEU420, PHE421, HIS432, TRP599, HIS600, ALA603 and ALA606 that make up the active site were used to build a grid. Zileuton was used as the reference. Docking scores as well as interaction residues of the reference molecule Zileuton and VS882, VS864, VS865, VS896, and VS898 (which were having high negative binding energies) are shown in table 3 From the docking analysis, it was found that hydrogen bonding interactions, and hydrophobic interactions are responsible for high negative binding energies of these molecules. Most of the compounds contained interactions with LEU368, ALA603, ALA410,

of the 18 compounds, as well as the ideal limits necessary for drug-like behaviour.

According to the findings, each molecule possesses most of the desirable characteristics of a drug molecule. All molecules contain more than 12 hydrogen bond acceptors, and molecules VS316, VS317, VS840, VS841 have 7 hydrogen bond donor sites, whereas molecules VS292, VS293, VS340, and VS341 have 8. Every molecule had a formal charge of either 0 or 1. It was discovered that the topological polar surface area (TPSA), which is the total of tabulated surface contributions of polar segments of all 18 molecules, was larger than 140. TPSA is an abbreviation for topologically polar surface area. The disintegration of the tablet or capsule is the initial stage in the drug absorption process, followed by the dissolving of the active medication. Low solubility makes excellent and full oral absorption difficult. The anticipated solubility (logS) of the following compounds was determined to be within the acceptable range of -4 to 5 logmol/L.

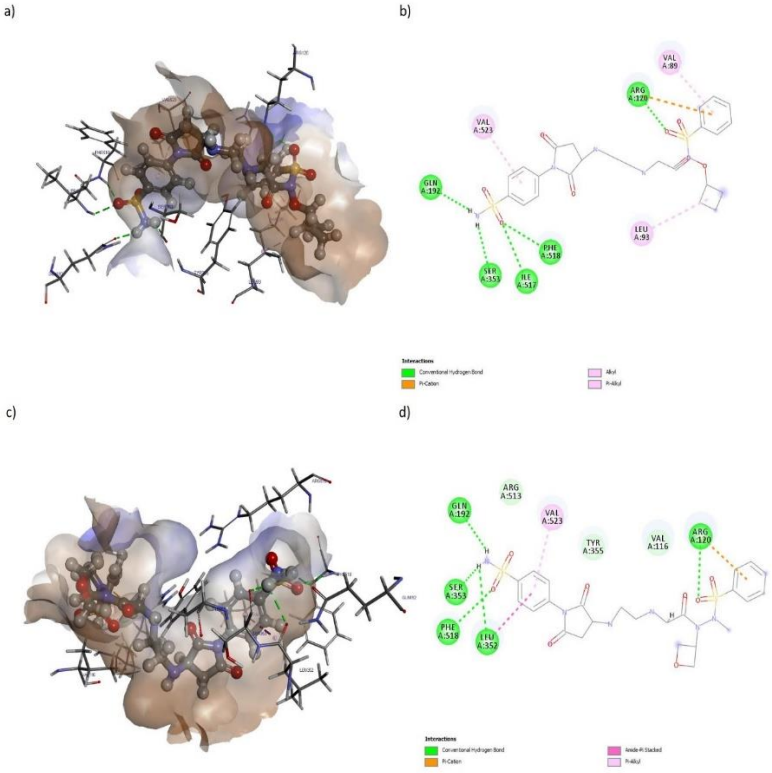

Figure 8: Docking pictures of ligands with COX-2 protein. a) 3D conformation of VS865 b) 2D interaction diagram of VS865 c) 3D conformation of VS896 and d) 2D interaction diagram of VS 896

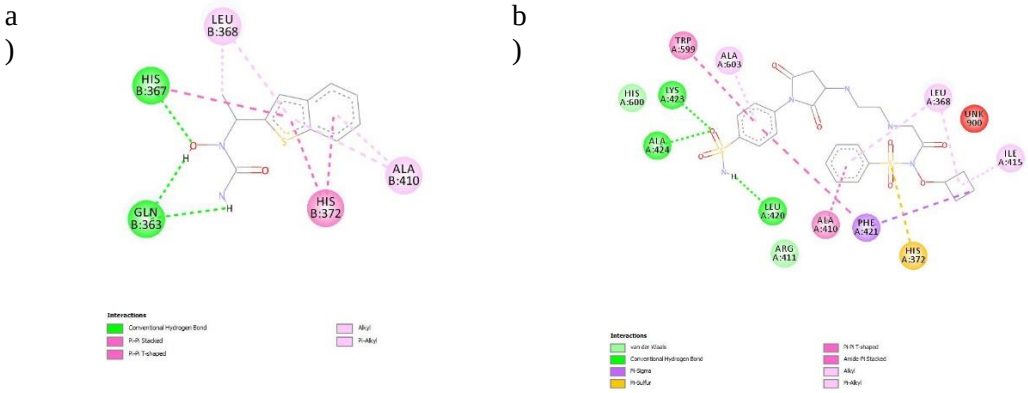

Figure 9: 2D interaction graphs of a) Zileuton and b) VS865 with 5-LOX protein.

Table 2: The docking score and the interacting residues of celecoxib and 18 molecules

Compound	Predicted pIC50	Docking score (kcal/mol)	Interacting residues
Celecoxib	*7.4	-10.78	SER 353, LEU352, HIS90, GLN192, ILE517, PHE518, TYR355, VAL349, ALA527, VAL523
VS292	7.52	-8.27	PHE518, LEU352, GLN192, TYR385, TRP387, VAL523
VS292	7.52	-8.81	PHE518, ILE517, SER353, LEU352, GLN192, TYR355, PRO86, VAL523, VAL89, ARG513
VS316	7.68	-8.53	TYR385, SER530, LEU352, ASP515, GLN192, LEU352, TRP387, HIS356
VS317	7.68	-8.52	ARG120, PHE518, ILE517, LEU352, HIS90, GLN192, VAL89, VAL523
VS340	7.5	-7.47	TYR385, SER530, SER353, TRP387, HIS95, GLY526, ALA527, VAL523, LEU352, HIS356, PRO514
VS341	7.5	-9.5	GLN192, SER353, ILE517, PHE518, ARG120, SER530, SER353, TYR385, VAL523, TRP387, TYR385
VS840	7.64	-9.13	ARG120, TYR355, PHE518, ILE517, SER353, LEU352, GLN192, LEU93, VAL523
VS841	7.64	-9.34	PHE518, GLN192, LEU352, HIS90, TYR355, ARG120, VAL89, LEU93, VAL523
VS864	7.5	-9.36	LEU352, GLN192, SER353, PHE518, ARG120, VAL89, LEU352, LEU93, VAL523
VS865	7.5	-9.76	ILE517, PHE518, SER353, GLN192, ARG120, VAL523, VAL89, LEU93
VS882	7.5	-8.52	ARG120, ILE517, PHE518, HIS90, ARG120, VAL89, LEU93, VAL323
VS884	7.5	-8.73	LEU352, SER353, ILE517, PHE518, GLN192, TYR115, LEU352, LEU93, VAL116, VAL523
VS888	7.82	-8.24	ARG120, ALA527, LEU93, VAL116, VAL523, ALA516, PHE518
VS889	7.82	-9.29	ARG120, HIS90, GLN192, LEU352, PHE518, ILE517, SER353, VAL89, LEU93, VAL523
VS895	7.5	-8.98	PHE518, SER353, LEU352, GLN192, TYR348, LEU352, LEU534, MET522, TRP387, PHE518, VAL523
VS896	7.5	-9.66	GLN192, SER353, PHE518, LEU352, ARG120, VAL523
VS897	7.5	-8.39	GLN192, PHE518, ILE517, ARG120, TYR115, LEU93, VAL89, VAL523
VS898	7.5	-9.27	ILE517, SER353, LEU352, PHE518, GLN192, ARG120, LEU93, VAL89, VAL523

* Estimated value

Table 3: The docking score and the interacting residues of zileuton and VS882, VS864, VS865, VS896, and VS898

Compound	Predicted pIC50	Docking score (kcal/mol)	Interacting residues	Interactions
Zileuton	*6.20	-8.74	HIS 367, GLN363, HIS372, ALA410, LEU368	Hydrogen bonding, alkyl/ pi-alkyl hydrophobic interactions, pi-pi T shaped interactions
VS864	5.81	-8.64	ASN425, ALA424, TRP599, HIS372, TYR181, LEU368, ILE415, ALA410, ARG411, ALA603	Hydrogen bonding, alkyl/ pi-alkyl hydrophobic interactions, T shaped pi-pi hydrophobic interactions, Pi-lone pair interactions
VS865	5.81	-8.86	LYS423, ALA424, LEU420, PHE421, TRP599, ALA410, LEU368, ILE415, ALA603	Hydrogen bonding, alkyl/ pi-alkyl hydrophobic interactions, amide-pi stacked / T shaped pi-pi hydrophobic interactions
VS882	6.15	-7.92	GLU376, GLN363, ALA410, PHE359, HIS367, ALA603, LEU368, TYR181	Hydrogen bonding, alkyl/ pi-alkyl hydrophobic interactions, pi-sigma interactions, amide-pi stacked / T shaped pi-pi hydrophobic interactions
VS896	6.15	-8.38	HIS367, ASN425, LYS423, ALA424, PHE421, TYR181, LEU368, ILE415, ALA603, HIS372	Hydrogen bonding, alkyl/ pi-alkyl hydrophobic interactions, pi-pi interactions, pi-sigma interactions
VS898	6.15	-8.58	LEU368, GLN557, GLN363, TRP599, PHE421, PHE177, ALA140, ILE406, PHE421, ALA603	Hydrogen bonding, alkyl/ pi-alkyl hydrophobic interactions, Pi-sulphur interactions, pi-pi T shaped interactions

* Estimated value

Table 4: Physicochemical properties of 18 virtually screened compounds

Compound	MW*	nHA*	nHD*	TPSA*	nRot*	fChar*	LogS	LogD 7.4	LogP	QED	SA score*	Lipinski	Pfizer
Desirable limits	**100 - 600**	**0-12**	**0-7**	**0-140**	**0-11**	**-4 to 4**	**-4 to 0.5 logmol/L**	**1 - 3 logmol/L**	**0 - 3 logmol/L**	**>0.67 : excellent**	**≤6: excellent**	**MW≤ 500; LogP ≤5; nHA ≤10; nHD ≤5**	**logP> 3; TPSA<75**
VS292	492.17	13	8	189.08	12	1	-3.228	-0.294	-0.721	0.157	3.978	Rejected	Accepted
VS293	506.18	13	8	189.08	12	1	-3.334	0.026	-0.391	0.157	3.955	Rejected	Accepted
VS316	492.17	13	7	178.22	12	1	-3.001	-0.06	-0.432	0.174	4.004	Rejected	Accepted
VS317	506.18	13	7	178.22	12	1	-3.079	0.221	-0.082	0.175	3.98	Rejected	Accepted
VS340	492.17	13	8	189.08	12	1	-2.964	0.232	-0.703	0.157	3.947	Rejected	Accepted
VS341	506.18	13	8	189.08	12	1	-3.075	0.601	-0.301	0.157	3.925	Rejected	Accepted
VS840	580.14	14	7	205.32	14	0	-3.581	0.659	-0.202	0.121	3.314	Rejected	Accepted
VS841	594.16	14	7	205.32	14	0	-3.693	1.014	-0.393	0.121	3.321	Rejected	Accepted
VS864	565.13	13	6	193.29	13	0	-3.66	0.18	-0.379	0.155	3.195	Rejected	Accepted
VS865	579.15	13	6	193.29	13	0	-3.773	0.506	-0.677	0.154	3.203	Rejected	Accepted
VS882	578.16	13	6	187.3	13	0	-3.616	0.253	-0.391	0.153	3.219	Rejected	Accepted
VS884	592.18	13	6	187.3	13	0	-3.713	0.567	-0.645	0.152	3.233	Rejected	Accepted
VS888	594.16	14	6	196.53	14	0	-3.571	0.73	-0.419	0.139	3.371	Rejected	Accepted
VS889	608.17	14	6	196.53	14	0	-3.695	1.078	-0.697	0.138	3.378	Rejected	Accepted
VS895	593.17	14	6	190.54	13	0	-3.035	0.126	-0.229	0.143	3.304	Rejected	Accepted
VS896	594.16	14	6	196.53	13	0	-3.508	0.104	-0.019	0.141	3.328	Rejected	Accepted
VS897	594.16	14	6	196.53	13	0	-3.384	0.28	-0.22	0.144	3.768	Rejected	Accepted
VS898	594.16	14	6	196.53	13	0	-3.384	0.28	-0.22	0.144	3.768	Rejected	Accepted

***MW**- Molecular weight; **nHA**- number of Hydrogen bond acceptors; **nHD**- number of Hydrogen bond donors, **TPSA**- Topological polar surface area; **nRot**- number of rotatable bonds; **fChar**-formal charge; **SA score**- Synthetic accessibility score

A medicine must enter the bloodstream and reach its target to be therapeutic. To dissolve in bodily fluid and permeate bio membranes, consumable medications must balance lipophilicity and hydrophilicity. In the early stages of drug discovery, it is necessary to measure n-octanol/water distribution coefficients at physiological pH (logD7.4) Except for VS292 and VS316 (LogD7.4: -0.294 and -0.06logmol/L), all other compounds exhibited suitable values. The outputs of the desirability functions based on the molecular weight (MW), the logP, the number of hydrogen bond acceptors (nHA), the number of hydrogen bond donors (nHD), TPSA, the number of rotatable bonds, the number of aromatic rings, and the number of alerts for undesirable functional groups are integrated to produce QED[35]. These molecules were the least suitable as drugs since their QED was less than 0.67 in all the compounds studied. According to the Lipinski rule, a drug-like molecule must meet the following criteria:

MW≤500; LogP≤5; nHA≤10; and nHD≤5. Poor absorption or permeability can occur when two characteristics are out of range. In this case, none of the compounds studied followed the Lipinski rule[36]. However, all compounds met the Pfizer criteria[37], which states that logP>3; TPSA<75 are

likely to be harmful. All the molecules in this area were inside the parameters. One of the most well-known common fitters is Pan Assay INterference compoundS (PAINS)[38], which consists of 480 substructures produced from the study of FHs determined by six target-based HTS assays. It is easy to screen false positive findings and identify problematic substances in screening databases using these filters. Because all 18 compounds have a PAINS score of zero, this implies that they are safe. Since all of the compounds have a synthetic accessibility score (SAscore)[39] of less than six, this suggests that it is not difficult to produce any of the molecules.

The anticipated absorption and distribution property scores of 18 virtually screened compounds are listed in table 5 by ADMETLab2.0. An oral medication must pass through intestinal cell membranes via passive diffusion, carrier-mediated absorption, or active transport pathways before reaching the systemic circulation. Due to their morphological and functional similarities, human colon adenocarcinoma cell lines (Caco2) are often employed to evaluate in vivo drug permeability. Because the score values for all 18 of the compounds are lower than -5.15log cm/s, it is possible that these are not suitable candidates for use as drugs. Because the score values for all 18 of the compounds are lower than -5.15log cm/s, it is possible that these are not suitable candidates for use as drugs. MDCK cells (Madin-Darby Canine Kidney Cells) have been established as an in vitro permeability model. Its apparent permeability coefficient P_{app} is commonly regarded as the gold standard for determining chemical updating effectiveness in the body in vitro. The influence of the Blood-Brain Barrier (BBB) is also estimated using P_{app} values from MDCK cell lines. In the present investigation, except for VS292, VS293, VS316, VS317, VS340, and VS341, all the other compounds exhibited outstanding MDCK permeability values. A compound is deemed to have high passive MDCK permeability when its P_{app} value is more than 2×10^{-6} cm/s.

Table 5: The anticipated absorption and distribution property scores of 18 virtually screened compounds

Compound	Caco-2	MDCK	HIA	F(20%)	BBB	PPB
Desirable limits	**>5.15: excellent**	**>2E-06: excellent**	**0-0.3: excellent 0.3-0.7:medium 0.7-1.0 poor**	**0-0.3: excellent 0.3-0.7:medium 0.7-1.0 poor**	**0-0.3: excellent 0.3-0.7:medium 0.7-1.0 poor**	**≤90%: excellent**
VS292	-6.038	1.33E-06	0.948	0.961	0.147	**33.52%**
VS293	-6.002	1.27E-06	0.937	0.97	0.155	29.55%
VS316	-6.159	1.32E-06	0.961	0.881	0.396	47.03%
VS317	-6.107	1.26E-06	0.95	0.911	0.381	44.89%
VS340	-6.058	1.35E-06	0.923	0.626	0.186	28.61%
VS341	-5.994	1.34E-06	0.913	0.707	0.183	25.14%
VS840	-6.763	4.74E-06	0.843	0.258	0.006	62.99%
VS841	-6.678	4.86E-06	0.831	0.193	0.005	64.88%
VS864	-6.285	4.36E-06	0.241	0.931	0.094	71.72%
VS865	-6.209	4.53E-06	0.163	0.931	0.074	74.60%
VS882	-6.824	3.67E-06	0.011	0.014	0.114	64.63%
VS884	-6.759	3.85E-06	0.012	0.018	0.085	67.23%
VS888	-6.621	4.34E-06	0.038	0.042	0.05	64.59%
VS889	-6.542	4.4E-06	0.035	0.042	0.043	66.27%
VS895	-6.686	2.39E-06	0.024	0.335	0.035	67.84%
VS896	-6.785	4.26E-06	0.012	0.233	0.105	64.76%
VS897	-6.78	4.36E-06	0.032	0.022	0.079	64.47%
VS898	-6.78	4.36E-06	0.032	0.022	0.079	64.47%

Oral medication effectiveness requires intestinal absorption. HIA (Human Intestinal Absorption) might be considered as an alternate measure for oral bioavailability because of the link between oral bioavailability and intestinal absorption. Less than 30% absorption is deemed poor. HIA>30% is found in VS864, VS865, VS882, VS884, VS888, VS889, VS895, VS896, VS897, and VS898. As a result, these compounds are suitable for usage as a medication. Human oral bioavailability is unquestionably one of the most significant pharmacokinetic criteria for any medicine delivered orally since it is an indicator of the efficacy of drug transport to the systemic circulation. Molecules with $F_{20\%}$ (the human oral bioavailability 20%) bioavailability were defined

as good for oral bioavailability, and VS840, VS841, VS882, VS884, VS888, VS889, VS895, VS896, VS897, and VS898 were determined to be orally bioavailable.

Plasma protein binding is a significant drug delivery method (PPB). Drug binding to plasma proteins affects pharmacodynamics. PPB can directly affect oral bioavailability because serum protein binding reduces free drug concentration. All 18 compounds have anticipated PPB values 90%, hence they have a valid PPB. To reach their molecular target, drugs that operate in the CNS must penetrate the blood-brain barrier (BBB). However, to prevent CNS adverse effects, drugs with peripheral targets may require minimal or no BBB penetration. VS316 and VS317 have a medium penetration probability, while all other compounds have a BBB+ possibility.

The process of drug metabolism reactions can be separated into (phase I) oxidative reactions and (phase II) conjugative reactions based on the chemical nature of bioinformation. The human cytochrome P450 family (phase I enzymes) has 57 isozymes, which metabolise nearly two-thirds of known pharmaceuticals in humans, with five isozymes -1A2,3A4,2C9,2C19, and 2D6 accounting for 80% of this. The liver contains the majority of the CYPs involved in phase I reactions. The metabolic activity score of all substances under evaluation was determined to be within the ideal range (excellent: 0-0.3). Table 6 depicts the predicted results of 18 virtually screened compounds. Except for VS292, VS293, VS316, VS317, VS340, and VS341, output values of 18 molecules were interpreted to have,$T_{1/2} \leq 3$. A drug's half-life is a composite term that includes clearance and distribution volume.

VS316 and VS317 were shown to be highly active in the hERG, whereas the rest were found to be moderately active. A voltage-gated potassium channel encoded by hERG plays a key function in the control of the interchange of cardiac action potential and resting potential during cardiac depolarization and repolarization. The hERG blockade can result in long QT syndrome and Torsade de Pointes (TdP), which can induce palpitations, fainting, and even death. Molecules with an IC50 more than 10μM or less than 50% inhibition at 10μM were categorised as hERG-, whereas those with an IC50 less than 10μM or more than 50% inhibition at 10μM were classified as hERG+. Drug-caused liver damage is a big safety concern for patients and a major reason why drugs are taken off the market. Based on the predicted toxicology results, the molecules were likely to be harmful to the liver (H-HT: the human hepatotoxicity value). The mutagenic effect is the most extensively used assay for assessing the mutagenicity of substances because it has a significant association with carcinogenicity. According to the AMES toxicity score value, VS864, VS865, VS882, VS884, VS895, VS896, VS897, and VS898 were expected to be less mutagenic. Because of its devastating impact on human health, carcinogenicity is one of the most important toxicological end points of chemical compounds. Chemicals may cause cancer by damaging the DNA or cellular metabolism. TD50 values are used to designate chemicals as carcinogenic or non-carcinogens. The chance of being harmful is represented by the output values, which range from 0 to 1. VS293, VS897, and VS898 were determined to be non-carcinogenic, whereas VS340, VS341, VS864, VS865, VS882, VS884, and VS896 were shown to have a medium carcinogenic potential.

Table 6: The anticipated metabolic properties and $T_{1/2}$ of 18 virtually screened substances

Compound	CYP1A2-inh	CYP2C19-inh	CYP2C9-inh	CYP2D6-inh	CYP3A4-inh	$T_{1/2}$
Desirable limits	**0 to 1**	**0 to 1**	**0 to 1**	**0 to 1**	**0 to 1**	**≤ 3**
VS292	0.013	0.031	0.03	0.092	0.034	**0.927**
VS293	0.015	0.034	0.041	0.131	0.045	0.927
VS316	0.035	0.117	0.111	0.472	0.026	0.923
VS317	0.042	0.134	0.175	0.573	0.037	0.924
VS340	0.002	0.028	0.01	0.005	0.013	0.82
VS341	0.003	0.029	0.011	0.008	0.018	0.797
VS840	0.008	0.024	0.068	0.012	0.062	0.194
VS841	0.011	0.027	0.118	0.018	0.114	0.186
VS864	0.017	0.026	0.338	0.022	0.141	0.272
VS865	0.021	0.029	0.483	0.044	0.249	0.252
VS882	0.004	0.022	0.121	0.002	0.232	0.202
VS884	0.004	0.024	0.178	0.004	0.449	0.178

VS888	0.009	0.026	0.212	0.002	0.14	0.226
VS889	0.011	0.029	0.299	0.004	0.261	0.202
VS895	0.004	0.018	0.037	0	0.126	0.207
VS896	0.002	0.016	0.069	0.001	0.095	0.288
VS897	0.003	0.018	0.072	0.001	0.08	0.323
VS898	0.003	0.018	0.072	0.001	0.08	0.323

Respiratory toxicity has been the leading cause of medication discontinuation among these safety concerns. Drug-induced respiratory toxicity is frequently misdiagnosed due to the lack of recognisable early signs or symptoms in popular drugs, and it can result in substantial morbidity and fatality. Therefore, thorough monitoring and treatment of respiratory toxicity are Endocrine disrupting chemicals (EDCs) impair the manufacture and normal activities of steroid hormones in the body, such as oestrogen and androgen. Aromatase catalyses the conversion of androgen to oestrogen and is important for the balance of androgen and oestrogen in several EDC-sensitive tissues. VS316, VS317, VS864, VS865, VS882, VS884, VS895, VS896, VS897, and VS898 have output values ranging from 0-0.3, showing that they are non-respiratory toxicants, whereas VS292, VS293, VS340, and VS341 had a medium range of respiratory toxicity.

Endocrine disrupting chemicals (EDCs) interfere with the biosynthesis and normal functions of steroid hormones including estrogen and androgen in the body. Aromatase catalyses the conversion of androgen to estrogen and plays a key role in maintaining the androgen and estrogen balance in many of the EDC-sensitive organs. In the present investigation, it was determined that no chemical could disrupt the equilibrium between androgen and oestrogen, as shown by its output value falling between 0.0 and 0.3. Estrogen receptor (ER), a nuclear hormone receptor, helps in development, metabolism, and reproduction. EDCs affect normal endocrine function by interacting with ER. It is vital to know how environmental pollutants affect ER signalling. The score value of 0-0.3 indicated that none of the chemicals under investigation might affect normal endocrine function. Oxidative stress causes cancer and neurodegeneration. ARE signalling being critical for treating oxidative damage. CellSensor ARE-bla HepG2 can study the Nrf2/antioxidant response signalling pathway (Invitrogen). Nrf2 and Nrf1 bind to and activate AREs. All the compounds tested were in the medium to active range. As a result, molecules may be risk-free. Because cancer cells reproduce fast, they must repeat their genome through DNA replication at each cell division. Failure to do so leads in the demise of cancer cells. Many chemotherapeutic drugs have been created based on this principle, however they have drawbacks such as limited effectiveness and significant side effects. Various forms of DNA damage led to an increase in Enhanced Level of Genome Instability Gene1(ELG1; human ATAD5) protein levels. All the proposed compounds are safe to use, according to ADMETLab 2.0's empirical conclusion (SR-ATAD5 score). Following DNA damage and other cellular stressors, the tumour suppressor protein p53 is activated. Activation of p53 controls cell destiny by causing DNA repair, cell cycle arrest, apoptosis, or senescence. Therefore, p53 activity is a reliable indication of DNA damage and other cellular stressors. All compounds under investigation were found to activate p53 in this manner. Heat shock response (HSR) activation can be triggered by a variety of substances, environmental stressors, and physiological stressors, and all the molecules under consideration are likely to do so. Toxicological study results were presented in table 7.

According to the results of the pharmacokinetic study, all the molecules were found to follow the Pfizer rule. The molecules VS864, VS865, VS882, VS884, VS895, VS896, VS897, and VS898 were found to be less hazardous and to have drug-like properties. These compounds have the potential to be used as therapeutic molecules in the future.

Molecular Dynamics Simulations

Since the protein is highly flexible conformational changes occurs will ligand binding which cannot be anticipated highly by molecular docking analysis. RMSD (Root Mean square deviation) analysis by molecular dynamics simulations aids in the estimation of repositioning of protein backbone upon formation of the docked complexes[40]. Eight hit compounds were subjected to MD analysis and RMSD values were compared with that of apoprotein. The protein and the ligands VS864, VS865, VS882, VS884, VS895, VS896, VS897, VS898 yielded average RMSDs of 2.09, 1.69, 1.91, 1.69, 1.69, 1.89, 1.16, 1.69 and 1.91 Å respectively. The RMSD plot is given in figure 10. Inspecting the figure, all the ligands reached a plateau after 17 ns. All the ligands have furnished

RMSDs less than the apoprotein leading to stable docked complexes.

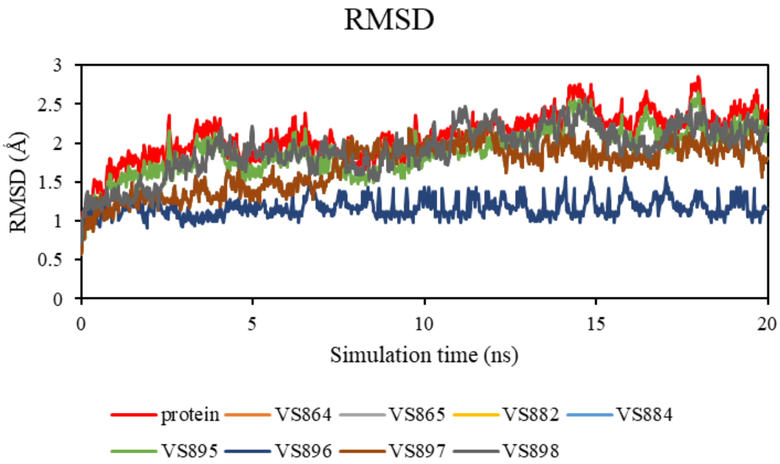

Figure 10: RMSD plot protein and docked complexes.

Table 7: Toxicological study results

Compound	hERG	H-HT	AMES	Carcinogenicity	Respiratory	NR-Aromatase	NR-ER	SR-ARE	SR-ATAD5	SR-HSE	SR-p53
Desired limits	**0-0.3: excellent 0.3-0.7: medium 0.7-1.0: poor**	**0-0.3: excellent 0.3-0.7: medium 0.7-1.0: poor**	**0-0.3: excellent 0.3-0.7: medium 0.7-1.0: poor**	**0-0.3: excellent 0.3-0.7: medium 0.7-1.0: poor**	**0-0.3: excellent 0.3-0.7: medium 0.7-1.0: poor**	**0-0.3: excellent 0.3-0.7: medium 0.7-1.0: poor**	**0-0.3: excellent 0.3-0.7: medium 0.7-1.0: poor**	**0-0.3: excellent 0.3-0.7: medium 0.7-1.0: poor**	**0-0.3: excellent 0.3-0.7: medium 0.7-1.0: poor**	**0-0.3: excellent 0.3-0.7: medium 0.7-1.0: poor**	**0-0.3: excellent 0.3-0.7: medium 0.7-1.0: poor**
VS292	0.386	0.652	0.707	0.019	0.444	0.194	0.065	0.543	0.008	0.005	0.37
VS293	0.398	0.672	0.701	0.02	0.487	0.278	0.066	0.595	0.008	0.007	0.393
VS316	0.23	0.752	0.996	0.884	0.231	0.012	0.081	0.223	0.004	0.001	0.029
VS317	0.242	0.759	0.996	0.879	0.238	0.017	0.082	0.249	0.004	0.001	0.029
VS340	0.609	0.809	0.635	0.435	0.52	0.02	0.164	0.587	0.009	0.004	0.369
VS341	0.62	0.818	0.621	0.462	0.552	0.028	0.171	0.64	0.009	0.005	0.391
VS840	0.426	0.952	0.987	0.933	0.855	0.01	0.276	0.649	0.005	0.003	0.122
VS841	0.439	0.953	0.986	0.932	0.856	0.013	0.283	0.685	0.005	0.004	0.13
VS864	0.407	0.897	0.024	0.519	0.042	0.012	0.209	0.382	0.003	0.001	0.023
VS865	0.42	0.898	0.024	0.507	0.045	0.015	0.214	0.416	0.003	0.001	0.025
VS882	0.668	0.979	0.017	0.344	0.241	0.004	0.118	0.51	0.003	0.002	0.005
VS884	0.665	0.977	0.017	0.302	0.267	0.005	0.121	0.543	0.003	0.002	0.005
VS888	0.446	0.964	0.968	0.902	0.813	0.021	0.17	0.539	0.004	0.003	0.038
VS889	0.462	0.965	0.966	0.895	0.817	0.025	0.174	0.579	0.004	0.003	0.041
VS895	0.582	0.99	0.239	0.914	0.803	0.002	0.08	0.209	0.003	0.001	0.002
VS896	0.526	0.961	0.022	0.527	0.074	0.006	0.121	0.375	0.003	0.002	0.006
VS897	0.543	0.973	0.016	0.209	0.093	0.006	0.14	0.498	0.004	0.002	0.007
VS898	0.543	0.973	0.016	0.209	0.093	0.006	0.14	0.498	0.004	0.002	0.007

Conclusion

The development of new computational processes in recent years has successfully defeated the old method of drug discovery, which is complex, expensive, and time-consuming. Both structure-based and ligand based virtual screening approaches can be used to identify hits and optimise leads for clinical drug development programmes in a sensible fashion. Prostaglandin and leukotrienes, two of the most important inflammatory mediators, are the focus of COX-2/5-LOX dual inhibitors' development. Our goal in this study was to use in silico methods to find COX-2/5-LOX dual inhibitors from a huge data set of 1022 compounds. 2D QSAR experiments on 63 COX-2/5-LOX inhibitor compounds were conducted initially with the goal of developing a convincing model for screening of powerful molecules as COX-2 and 5-LOX dual inhibitors. After conducting several statistical analyses with

fingerprints, as well as 2D and 3D molecular descriptors, we were able to develop statistically reliable QSAR models for COX-2 inhibition and 5-LOX inhibition. As a result, highly predictive models were created, each of which exhibited a high degree of correlation with the training set as well as the test set ($R^2 = 0.9308$ and $Q^2 = 0.8936$ for COX-2 inhibition and $R^2 = 0.9209$ and $Q^2 = 0.8879$ for 5-LOX inhibition). The cross validated R^2 value and Y scrambling values were used to determine the models' effectiveness. The models were then used to screen new derivatives (1022). 18 compounds had a predicted pIC50 value that was higher than 7.5 out of a total of 1022 molecules. The docking study of these compounds was then performed using celecoxib as a reference. The presence of hydrophobic contacts and hydrogen bonding connections enhance inhibitory activity, according to the findings. Hydrophobic interactions with LEU93, VAL89, VAL349, and LEU352, as well as hydrogen bonding interactions with PHE518, GLN192, SER353, ILE517, LEU352 and ARG120, were found to be prevalent in active compounds for COX-2 inhibition. In active compounds for 5-LOX inhibition, it was revealed that hydrogen bonding interactions with GLN363 and hydrophobic interactions with LEU368, ALA603, and ALA410 were frequent. All 18 compounds under consideration were chosen for pharmacokinetic investigations because they all showed a significant degree of interaction with the target protein. In accordance with all the most recent recommendations for drug likeness, the pharmacokinetic features together with the ADMET study demonstrates that VS864, VS865, VS882, VS884, VS895, VS896, VS897, and VS898 might be considered the best molecules because they don't have any potentially harmful effects. The binding stability and conformational changes connected to the protein ligand complexes of these top eight chemicals were revealed by molecular dynamics investigations. As a result, it is possible that these compounds could be used as promising candidates in the development of powerful COX-2/5-LOX dual inhibitors.

Acknowledgements
The authors would like to thank University of Kerala for comprehending this research work. We owe a special thanks to Dr. A Muhammed Thaha, Principal, Milad-E-Sherief Memorial College in Kayamkulam, who has been supportive of our professional objectives and has worked hard to ensure that we have the protected academic time we need to pursue them.

Conflict of Interest
The authors declares that there is no conflict of interest.

Funding Sources
There are no funding sources.

References
1. Marsico, Fabio; Paolillo, Stefania; Filardi, P. P. NSAIDs and cardiovascular risk. *J. Cardiovasc. Med.* **18**, e40–e43 (2017).
2. Jacqueline K.InnesaPhilip C.Caldera. Omega-6 fatty acids and inflammation. *Prostaglandins, Leukot. Essent. Fat. Acids* **132**, 41–48 (2018).
3. Meshram, M. A., Bhise, U. O., Makhal, P. N. & Kaki, V. R. Synthetically-tailored and nature-derived dual COX-2/5-LOX inhibitors: Structural aspects and SAR. *Eur. J. Med. Chem.* **225**, 113804 (2021).
4. Jaismy Jacob, P. & Manju, S. L. Novel approach of multi-targeted thiazoles and thiazolidenes toward anti-inflammatory and anticancer therapy—dual inhibition of COX-2 and 5-LOX enzymes. *Med. Chem. Res.* **30**, 236–257 (2021).
5. Gaganpreet Kaur, O. S. Multiple target-centric strategy to tame inflammation. *Future Med. Chem.* **9**, 1361–1376 (2017).
6. C.A.C.HydeS.Missailidis. Inhibition of arachidonic acid metabolism and its implication on cell proliferation and tumour-angiogenesis. *Int. Immunopharmacol.* **9**, 701–715 (2009).
7. Shaaban, M. A. *et al.* Design, synthesis, and biological evaluation of new pyrazoloquinazoline derivatives as dual COX-2/5-LOX inhibitors. *Arch. Pharm. (Weinheim).* **353**, (2020).
8. Gedawy, E. M., Kassab, A. E. & El Kerdawy, A. M. Design, synthesis and biological evaluation of novel pyrazole sulfonamide derivatives as dual COX-2/5-LOX inhibitors. *Eur. J. Med. Chem.* **189**, 112066 (2020).
9. Jaismy JacobP,S.L.Manju, K.R.Ethiraj, G. Safer anti-inflammatory therapy through dual COX-2/5-LOX inhibitors: A structure-based approach. *Eur. J. Pharm. Sci.* **121**, (2018).
10. S. Tries, W. N. & S. L. The mechanism of action of the new antiinflammatory compound ML3000: inhibition of 5-LOX and COX-1/2. *Inflamm. Res. Vol.* **51**, 135–143 (2002).
11. Sabe, V. T. *et al.* Current trends in computer aided drug design and a highlight of drugs discovered via computational techniques: A review. *Eur. J. Med. Chem.* **224**, 113705 (2021).
12. Masand, V. H. *et al.* Does tautomerism

influence the outcome of QSAR modeling? *Med. Chem. Res.* **23**, 1742–1757 (2014).
13. David C. Young. *Computational Drug Design-A guide for Computational and Medicinal Chemists*. (Wiley Publications, 2009).
14. Palacios, J. Computer Aided Design of Drug Delivery Systems.
15. van de Waterbeemd, H. & Gifford, E. ADMET in silico modelling: Towards prediction paradise? *Nat. Rev. Drug Discov.* **2**, 192–204 (2003).
16. Ntie-Kang, F. *et al.* In silico drug metabolism and pharmacokinetic profiles of natural products from medicinal plants in the Congo basin. *silico Pharmacol.* **1**, 12 (2013).
17. Kitchen, D. B., Decornez, H., Furr, J. R. & Bajorath, J. Docking and scoring in virtual screening for drug discovery: Methods and applications. *Nat. Rev. Drug Discov.* **3**, 935–949 (2004).
18. Xuan-Yu Meng, Hong-Xing Zhang, Mihaly Mezei, and M. C. Molecular Docking: A powerful approach for structure- based drug discovery. *Curr. Comput. Aided Drug Des.* **7**, 146–157 (2012).
19. Javed, M. A. *et al.* Structural Modification, in Vitro, in Vivo, Ex Vivo, and in Silico Exploration of Pyrimidine and Pyrrolidine Cores for Targeting Enzymes Associated with Neuroinflammation and Cholinergic Deficit in Alzheimer's Disease. *ACS Chem. Neurosci.* **12**, 4123–4143 (2021).
20. Sajjad Ahmad, Mater H Mahnashi, Bandar A Alyami, Yahya S Alqahtani, farhat Ullah, Muhammad Ayaz, Muhammad Tariq, Abdul Sadiq, U. R. Blocks for Potential Analgesic Drugs: In vitro, in vivo and in silico Explorations. *Drug Des. Devel. Ther.* **15**, 1299–1313 (2021).
21. Sadiq, A. *et al.* Tailoring the substitution pattern of Pyrrolidine-2,5-dione for discovery of new structural template for dual COX/LOX inhibition. *Bioorg. Chem.* **112**, (2021).
22. Munir, A. *et al.* Synthesis, in-vitro, in-vivo anti-inflammatory activities and molecular docking studies of acyl and salicylic acid hydrazide derivatives. *Bioorg. Chem.* **104**, (2020).
23. Jan, M. S. *et al.* Design, synthesis, in-vitro, in-vivo and in-silico studies of pyrrolidine-2,5-dione derivatives as multitarget anti-inflammatory agents. *Eur. J. Med. Chem.* **186**, (2020).
24. Yap, C. W. PaDEL-descriptor: An open source software to calculate molecular descriptors and fingerprints. *J. Comput. Chem.* **32**, 1466–1474 (2010).
25. Gramatica, P., Chirico, N., Papa, E., Cassani, S. & Kovarich, S. QSARINS : A New Software for the Development , Analysis , and Validation of QSAR MLR Models. *J. Comput. Chem.* **34**, 2121–2132 (2013).
26. Gramatica, P., Cassani, S. & Chirico, N. QSARINS-Chem : Insubria Datasets and New QSAR / QSPR Models for Environmental Pollutants in QSARINS. *J. Comput. Chem.* **35**, 1036–1044 (2014).
27. Schrodinger Release 2021-1.
28. Garrett M. Morris,Ruth Huey, A. J. O. Using AutoDock for Ligand-Receptor Docking. *Curr. Protoc. Bioinforma.* **24**, 8–14 (2008).
29. Diego de Sousa Miranda. Python: a programming language for soware integration and development. *J Mol Graph Model* **17**, 57–61 (1999).
30. Orlando, B. J. & Malkowski, M. G. Crystal structure of rofecoxib bound to human cyclooxygenase-2. *Acta Crystallographica Section:F Structural Biology Communications* vol. 72 772–776 (2016).
31. Nathaniel C Gilbert, Sue G Bartlett, Maria T Waight, David B Neau, William E Boeglin, Alan R Brash, M. E. N. The structure of human 5-lipoxygenase. *Science (80-.).* **331**, 217–219 (2011).
32. Guoli Xiong, Zhenxing Wu, Jiacai Yi, Li Fu, Zhijiang Yang, Changyu Hsieh, Mingzhu Yin, Xiangxiang Zeng, Chengkun Wu, Aiping Lu, Xiang Chen, T. H. ADMETlab 2.0: an integrated online platform for accurate and comprehensive predictions of ADMET properties. *Nucleic Acids Res.* **49**, W5-w14 (2021).
33. Phillips JC, Hardy DJ, Maia JD, Stone JE, Ribeiro JV, Bernardi RC, Buch R, Fiorin G, Hénin J, Jiang W, M. R. Scalable molecular dynamics on CPU and GPU architectures with NAMD. *J. Chem. Phys.* **153**, 044130 (2020).
34. Yamada Y, Gohda S, Abe K, Togo T, Shimano N, Sasaki T, Tanaka H, Ono H, Ohba T, Kubo S, O. T. Carbon materials with controlled edge structures. *Carbon N. Y.* **122**, 694–701 (2017).
35. G. Richard Bickerton, Gaia V. Paolini, Jérémy Besnard, S. M. & A. L. H. Quantifying the chemical beauty of drugs. *Nat. Chem.* **4**, 90–98 (2012).
36. Christopher A.LipinskiFrancoLombardoBeryl W.DominyPaul J.Feeney. Experimental and computational approaches to estimate solubility and permeability in drug discovery and development settings. *Adv. Drug Deliv. Rev.* **23**, 3–25 (1997).
37. Hughes, J. D. *et al.* Physiochemical drug

properties associated with in vivo toxicological outcomes. *Bioorganic Med. Chem. Lett.* **18**, 4872–4875 (2008).
38. Baell, J. B. & Holloway, G. A. New substructure filters for removal of pan assay interference compounds (PAINS) from screening libraries and for their exclusion in bioassays. *J. Med. Chem.* **53**, 2719–2740 (2010).
39. Ertl, P. & Schuffenhauer, A. Estimation of synthetic accessibility score of drug-like molecules based on molecular complexity and fragment contributions. *J. Cheminform.* **1**, 1–11 (2009).
40. Achutha AS, Pushpa VL, S. S. Theoretical insights into the anti-SARS-CoV-2 activity of chloroquine and its analogs and in silico screening of main protease inhibitors. *J. Proteome Res.* **19**, 4706–17 (2020).